

Supporting Information

Spatial catalytic acid-base-Pd triple-sites of a hierarchical core-shell structure for three-step tandem reaction

Jian Wu,^a Gang-Gang Chang,^{*a} You-Qing Peng,^a Xiao-Chen Ma,^a Shan-Chao Ke,^a Si-Ming Wu,^a Yu-Xuan Xiao,^a Ge Tian,^{*a} Tao Xia^a and Xiao-Yu Yang^{*a, b}

^a School of Chemistry, Chemical Engineering and Life Science and State Key Laboratory of Advanced Technology for Materials Synthesis and Processing, Materials Science & Engineering, Wuhan University of Technology, 122, Luoshi Road, 430070, Wuhan, Hubei, China.

^b Qingdao National Laboratory for Marine Science and Technology, Qingdao, 266237, China.

Author Contributions

J. W., Y. Q. P., X. C. M. and S. C. K. did the experiments of synthesis and catalytic performance. X. Y. Y. and G. G. C. conceived the project, provided the idea, and designed the experiments. G. T. helped with the TEM measurements and corresponding analysis. X. Y. Y., G. G. C. and J. W. wrote and revised the paper. S. W. W., Y. X. X. and T. X. revised the paper. All the authors discussed results and analyzed the data.

EXPERIMENTAL SECTION

1. Chemicals

Zn(NO₃)₂·6H₂O (98%, Aladdin), 2-methylimidazole (2-MeIM, 99%, Aladdin), Na₂PdCl₄ (Pd 34.7%, Aladdin), benzaldehyde dimethyl acetal (98%, Aladdin), cetyltrimethylammonium bromide solution (CTAB, 25 mg mL⁻¹, Aladdin), tetraethyl orthosilicate (TEOS, ≥99%, Aladdin), dodecane (98%, Aladdin), malonitrile (99%, Aladdin), phosphotungstic acid hydrate (PTA, H₃O₄₀PW₁₂·xH₂O, Aladdin), N,N-

dimethylformamide (DMF) and other organic solvents were purchased from Sinopharm Chemical. All of the chemicals used in this experiment were used as received without further purification.

2. Synthesis of hierarchical core-shell structured catalysts

Synthesis of ZIF-8: The fabrication of ZIF-8 was according to a previously published method with minor revision. Specifically, 3.36 g of $\text{Zn}(\text{NO}_3)_2 \cdot 6\text{H}_2\text{O}$ was first dissolved into 160 mL methanol. Then, a mixture of 7.40 g of 2-MeIM with 160 mL methanol was added under stirring for 24 h at room temperature. Finally, the obtained product was separated and washed thoroughly by methanol, and dried at 80 °C overnight under high vacuum.

Synthesis of $\text{Pd}^{2+}@ZIF-8$: The $\text{Pd}^{2+}@ZIF-8$ was synthesized via a simple impregnation method. Taking the synthesis of 1.12 wt% $\text{Pd}^{2+}@ZIF-8$ as an example, 100 mg of dried ZIF-8 was well-dispersed in 5 mL of pure water under sonication. Then, an aqueous solution (62.3 μL) including 2.76 mg of Na_2PdCl_4 was added dropwise to the above solution and stirred for additional 12 h at room temperature. Finally, the impregnated ZIF-8 was washed thoroughly with water and dried at 80 °C for 8 h under high vacuum. The Pd^{2+} loading amount could be tuned by changing the mass ratio of palladium precursor/MOF during fabrication process.

Preparation of $\text{Pd}^{2+}@ZIF-8@SiO_2$: The encapsulation procedure of mesoporous SiO_2 was prepared according to previously reported method. Briefly, a certain amount of $\text{Pd}^{2+}@ZIF-8$ (600 mg) was well-dispersed in 240 mL of H_2O , which was added to 6 mL aqueous CTAB and 9.6 mL NaOH solution. Then, TEOS (1.2 mL in 6 mL of methanol) was injected into the above mixture, and stirred for another 3 h. The resulted $\text{Pd}^{2+}@ZIF-8@SiO_2$ core-shell structured composites were separated and washed with ethanol, and further dried under high vacuum.

Preparation of $\text{Pd}@N-ZDC@mSiO_2$: The as-prepared $\text{Pd}^{2+}@ZIF-8@SiO_2$ was transferred to a tube furnace and was pyrolysed under Ar atmosphere at 800 °C for 3 h. Then the obtained black products were cooled down naturally, during which, the ZIF-8 was evolved into nitrogen doped ZIF-8 derived porous carbon (N-ZDC), the

Pd^{2+} was in-situ reduced to Pd NPs, and template CTAB was also removed to expose uniform mesopore. The final obtained product was referred to $\text{Pd}@N\text{-ZDC}@m\text{SiO}_2$.

Preparation of $\text{Pd}@N\text{-ZDC}@PTA\text{-}m\text{SiO}_2$: The $\text{Pd}@N\text{-ZDC}@m\text{SiO}_2$ was dispersed in 10 mL of H_2O , and then a certain amount of PTA (20 mg) was added. The sample was stirred at room temperature for 5 h. Then, the resulted $\text{Pd}@N\text{-ZDC}@PTA\text{-}m\text{SiO}_2$ core-shell structured products were separated and washed thoroughly with ethanol and water alternatively for three times. PTA content was revealed by ICP-OES analysis. After loading and washing, we firstly determined the content of P and W through ICP test, and then calculated the loading of phosphotungstic acid by its molecular mole ratio. In order to demonstrate the effectiveness of the hierarchically porous core-shell structured multifunctional catalyst $\text{Pd}@N\text{-ZDC}@PTA\text{-}m\text{SiO}_2$ toward the D-K-H reaction, catalysts of $\text{Pd}@N\text{-ZDC}@m\text{SiO}_2$, $N\text{-ZDC}@m\text{SiO}_2$ and $N\text{-ZDC}@PTA\text{-}m\text{SiO}_2$ without acid sites, base sites, metal sites and several sample without hierarchically porous core-shell nanostructure were also synthesized as well for systematically comparison.

Preparation of contrast sample with thick shell: The same step was used to fabricate contrast $N\text{-ZDC}@PTA\text{-}m\text{SiO}_2$ catalyst with thick $m\text{SiO}_2$. When coated with SiO_2 , ZIF-8 (600 mg) was well-dispersed in 240 mL of H_2O , which was added to 6 mL aqueous CTAB and 19.2 mL NaOH solution. Then, TEOS (2.4 mL in 12 mL of methanol) was injected into the above mixture, and stirred for another 3 h. The resulted $\text{ZIF-8}@SiO_2$ composites with core-shell structure was separated and washed with ethanol, and further dried under high vacuum. After calcined under Ar atmosphere at 800 °C for 4 h and loaded PTA using same method, the contrast sample $N\text{-ZDC}@PTA\text{-}m\text{SiO}_2$ (thick shell) was obtained.

3. General procedure for three-step tandem reaction

Benzaldehyde dimethyl acetal (0.3 mmol), malononitrile (1.2 mmol), and 20 mg of catalyst were well-dispersed in 8 mL solvent. The tandem reaction was first carried out in a Schlenk tube (25 mL) at 80 °C under stirring for 24 h. After the reaction was completed, the solution was transferred to a stainless-steel autoclave, which was

sealed and repeatedly flushed with H₂ for five times. The hydrogenation reaction was performed in 0.2 MPa H₂ at 80 °C for 24 h. Other contrast reaction adopted similar mole ratio. After finished, the product was separated and determined by gas chromatography (GC, Agilent 7890B) equipped with a HP-5ms capillary column (30 m × 0.32 mm × 0.25 μm) using dodecane as an internal standard. To evaluate the catalytic reusability and stability of Pd@N-ZDC@PTA-mSiO₂, after each run, the catalyst was isolated and thoroughly washed with ethanol, and then reused in the next run with the same reaction conditions described above.

4. Characterization

The surface morphology of catalysts observation was carried out on a field emission scanning electron microscope (FESEM, S-4800, HITACHI) and a transmission electron microscope (TEM, Talos F200S). The power X-ray diffraction (XRD) patterns were measured on an X-ray diffractometer with Cu K α radiation (D8 Advance, Bruker, $\lambda=1.5418$ Å). The N₂ adsorption-desorption isotherms at 77 K were measured on a surface area analyzer Tristar II 3020. ICP measurements were operated on inductively coupled plasma-atomic emission spectroscopy (ICP-AES, Prodigy7). Fourier transform infrared spectroscopy (FT-IR) spectra were performed using a Bruker VerTex 80 v spectrometer. X-ray photoelectron spectroscopy (XPS) measurements were performed on a PHI Quantera II, (ULVAC-PHI, Japan) for chemical composition analysis. CO₂-TPD and NH₃-TPD experiments were performed on a home-made TPD apparatus with default program for the instruments.

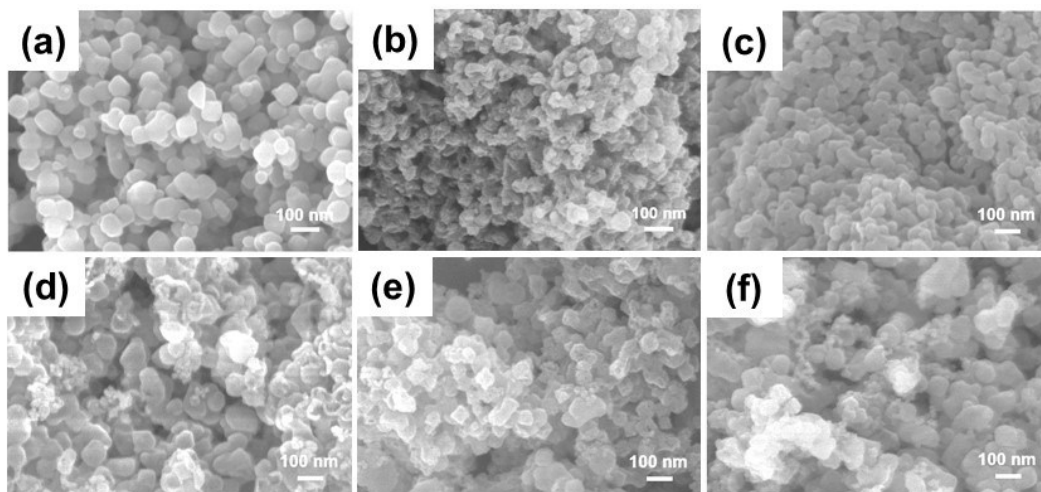


Figure S1. The SEM images of the as-prepared (a) Pd²⁺@ZIF-8, (b) Pd@N-ZDC, (c) Pd²⁺@ZIF-8@SiO₂, (d) Pd@N-ZDC@PTA-mSiO₂, (e) 0.15 wt% Pd@N-ZDC@PTA-mSiO₂, (f) 2.87 wt% Pd@N-ZDC@PTA-mSiO₂.

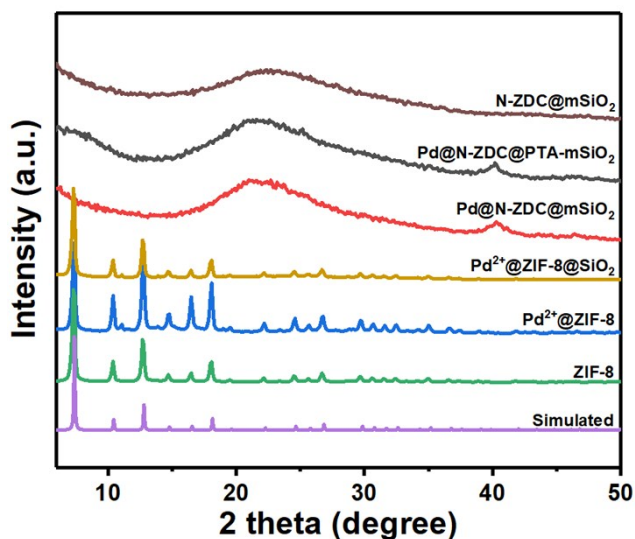


Figure S2. (a) Powder XRD patterns of simulated ZIF-8, as-synthesized ZIF-8 and nanostructured catalysts during different synthetic process.

Detailed description for XRD:

The composition and structural evolution of different catalyst sample were measured by X-ray powder diffraction (XRD). Compared with the standard XRD pattern of ZIF-8, the as-synthesized ZIF-8, Pd²⁺@ZIF-8 and Pd²⁺@ZIF-8@SiO₂ all showed similar patterns and matched well with the simulated one, which indicated that ZIF-8 was successfully synthesized and the introduction of Pd²⁺ and the coating of SiO₂ on ZIF-8 had no harm for the crystallinity of ZIF-8. When the Pd²⁺@ZIF-8@SiO₂ was pyrolyzed to form hierarchically porous Pd@N-ZDC@mSiO₂, the typical peaks of ZIF-8 crystal disappeared and a new peak at around 23° appeared which was ascribed to the carbon (002) diffraction indicating the evolution of crystalline ZIF-8 to an amorphous carbon material. Notably, a new and weak reflex peak at about 40° was also observed, which could be assigned to the metallic Pd NPs.

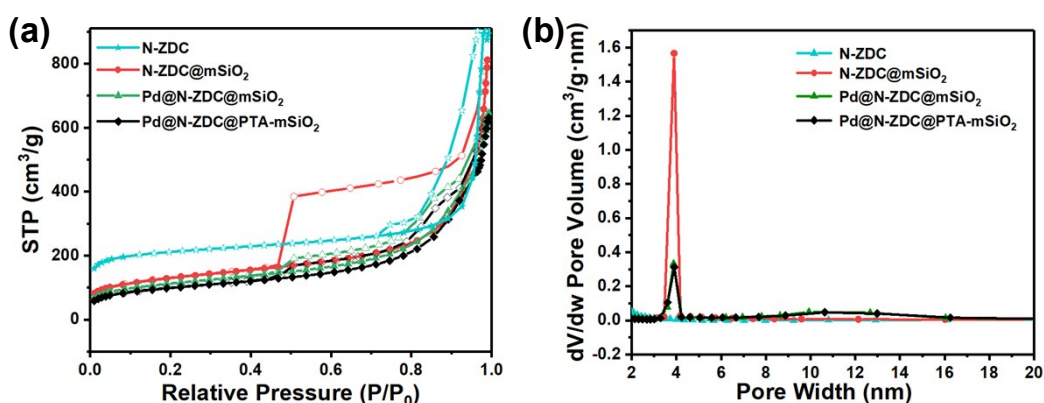


Figure S3. (a) N₂ adsorption-desorption isotherms of N-ZDC, N-ZDC@mSiO₂, Pd@N-ZDC@mSiO₂, Pd@N-ZDC@PTA-mSiO₂ and (b) the corresponding pore size distribution profiles calculated from the adsorption branch in the isotherm curves by the BJH method.

Detailed description for N₂ adsorption-desorption isotherms:

The hierarchical porosity in the core-shell structured catalysts was then characterized by N₂ adsorption isotherms at 77 K. after being coated with mSiO₂, N-ZDC@mSiO₂ exhibited an IV-type curve with a hysteresis loop observed in the relative pressure range of 0.45 ~ 0.9, which indicated the hierarchical micro-/mesopore in N-ZDC@mSiO₂. The BET specific surface area (Table S1) of N-ZDC@mSiO₂ was about 448 m²/g and gradually decreased to 391 m²/g (Pd@N-ZDC@mSiO₂) and 343 m²/g (Pd@N-ZDC@PTA-mSiO₂) after the encapsulation of metal sites and PTA molecule in sequence. On the contrary, N-ZDC derived from pure ZIF-8 sample showed type I curve and owned 800 m²/g BET specific surface area, which was characteristic of microporous materials. The hysteresis loop occurred at relatively high pressure (0.85 ~ 1) mainly resulted from the accumulation of NPs.

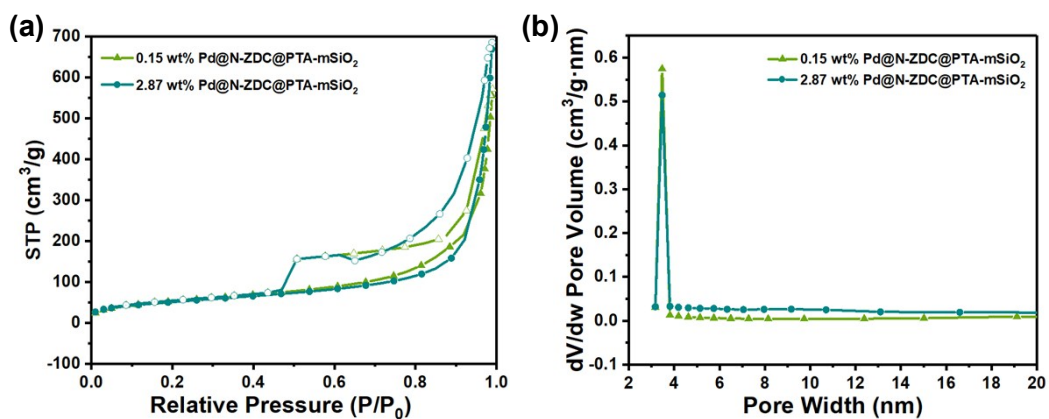


Figure S4. N_2 adsorption-desorption isotherms of (a) 0.15 wt% Pd@N-ZDC@PTA-mSiO₂, 2.87 wt% Pd@N-ZDC@PTA-mSiO₂, and (b) the corresponding pore size distribution profiles calculated from the adsorption branch in the isotherm curves by the BJH method.

Table S1. BET surface area and pore volume of N-ZDC, N-ZDC@mSiO₂, Pd@N-ZDC@mSiO₂, Pd@N-ZDC@PTA-mSiO₂, 0.15 wt% Pd@N-ZDC@PTA-mSiO₂, 2.87 wt% Pd@N-ZDC@PTA-mSiO₂.

Entry	Sample	BET (m²g⁻¹)	Pore Volume (cm³g⁻¹)
1	N-ZDC	800	1.11
2	N-ZDC@mSiO ₂	448	1.26
3	Pd@N-ZDC@mSiO ₂	391	11.71
4	Pd@N-ZDC@PTA-mSiO ₂	343	0.94
5	0.15 wt% Pd@N-ZDC@PTA-mSiO ₂	191	0.85
6	2.87 wt% Pd@N-ZDC@PTA-mSiO ₂	184	1.04

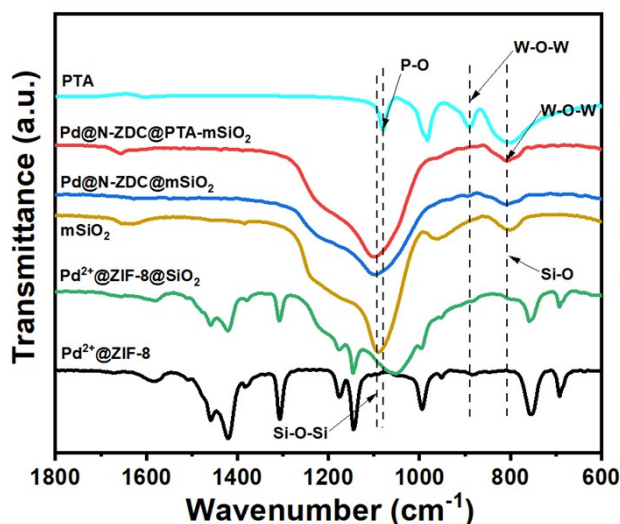


Figure S5. FT-IR spectra of nanostructured catalysts during different synthetic stage and the contrast sample of mSiO₂ and PTA

Detailed description for FT-IR:

Pd²⁺@ZIF-8 composite showed similar FT-IR spectra to the initial ZIF-8. In the spectrum of mSiO₂, Pd@N-ZDC@mSiO₂, and Pd@N-ZDC@PTA-mSiO₂, the appearance of Si-O-Si antisymmetric stretching vibration absorption peak at 1093 cm⁻¹ and Si-O symmetrical stretching vibration absorption peak at 807 cm⁻¹ compared to pure ZIF-8 and Pd²⁺@ZIF-8 represented the successful coating of mSiO₂ on the inner core. Besides, the characteristic absorption peak for ZIF-8 almost disappeared after high temperature calcination, indirectly identifying the structure transformation. Notably, for Pd²⁺@ZIF-8@SiO₂, the characteristic absorption peak of silica shifted toward low wavenumber (1054 cm⁻¹) which might be due to the electron conjugation effects resulted from the existence of imidazole ring in ZIF-8. Meanwhile, the characteristic peaks of PTA molecule which showed the vibrations of P-O, terminal W=O, corner sharing W-O-W bonds, and edge sharing W-O-W at around 1083, 985, 808, and 893 cm⁻¹ respectively were presented clearly in FT-IR spectra. These peaks were also observed in the Pd@N-ZDC@PTA-mSiO₂ composites. The characteristic peaks of both PTA and mSiO₂ found in the IR spectra of Pd@N-ZDC@PTA-mSiO₂ composites further demonstrated the successful incorporation of the PTA molecule into the mSiO₂ shell of core-shell structured nanocatalyst.

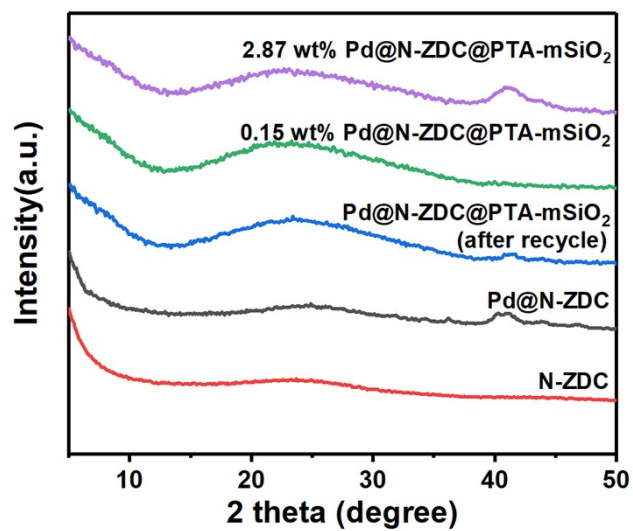


Figure S6. Powder XRD patterns of N-ZDC, Pd@N-ZDC, Pd@N-ZDC@PTA-mSiO₂ after five times recycling and Pd@N-ZDC@PTA-mSiO₂ with different Pd loading.

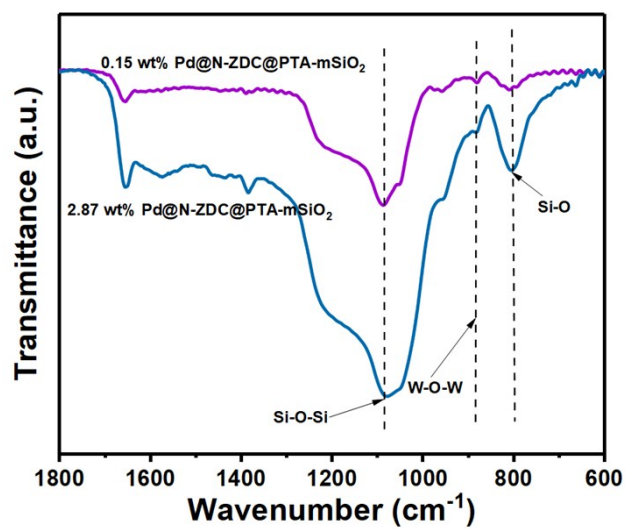


Figure S7. FT-IR spectra of 0.15 wt% Pd@N-ZDC@PTA-mSiO₂, 2.87 wt% Pd@N-ZDC@PTA-mSiO₂.

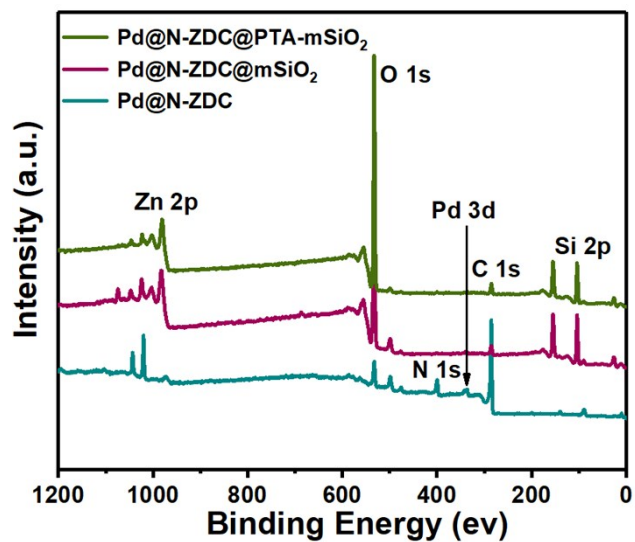


Figure S8. Survey XPS spectra of Pd@N-ZDC, Pd@N-ZDC@mSiO₂, Pd@N-ZDC@PTA-mSiO₂.

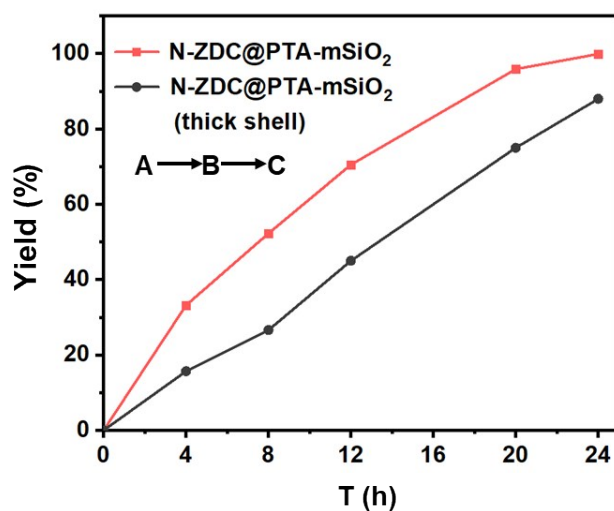


Figure S9. Two step reactions with N-ZDC@PTA-mSiO₂ and N-ZDC@PTA-mSiO₂ (thick shell) catalysts. The reaction kinetic constants (K) were 4.76 and 3.69 by calculated the two-step reaction from benzaldehyde dimethyl acetal (raw material A) to benzylidenemalononitrile (product C) using N-ZDC@PTA-mSiO₂ and N-ZDC@PTA-mSiO₂ (thick shell) catalysts respectively.

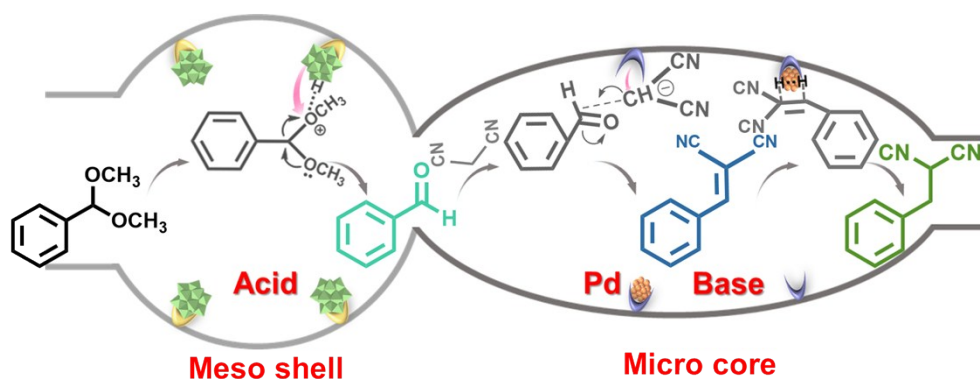


Figure S10. Schematic illustration of the three-step tandem reaction catalyzed by hierarchical Pd@N-ZDC@PTA-mSiO₂.

Detailed description for reaction mechanism:

Based on the catalytic results, a possible reaction mechanism was proposed for the three-step D-K-H reactions, which was illustrated detailed in figure S10. To be brief, firstly, the methoxy group of benzaldehyde dimethyl acetal got activated by the surface acidic sites via capturing H⁺ ions to proceed as the Lewis acid site which allowed nucleophilic attack by adjacent O, leading to the broken of C-O bond and the following generation of benzaldehyde. Then, the N species as base sites within the multifunctional catalyst detached an acidic proton of the methylene group of malononitrile, giving a carboanion, which acted as a role of nucleophile to react with the carbonyl group of benzaldehyde to give the benzylidenemalononitrile after dehydration. Finally, both of the resulted benzylidenemalononitrile and added hydrogen were adsorbed and activated on the surface of supported Pd NPs to form the active hydrogen atom and the open of the double bond. After the hydrogen atoms from the dissociation of H₂ were added to benzylidenemalononitrile, the final product was obtained. The spatial catalytic acid-base-Pd triple-sites of the hierarchical core-shell structure was very favor to three-step tandem reaction. In tandem catalysis, each acid, base and Pd sites were essential to drive the one, two and three step reactions. The hierarchical micro-core@meso-shell structure played an important role in yielding the final target product. The all results have been conducted to study the

spatial catalytic acid-base-Pd triple-sites and its marvellous specialties, such as: (i) spatial confinement and distribution of catalytic sites; (ii) outside-in order of acid-base-Pd for corresponding reaction order; (iii) hierarchical microporous core@mesoporous shell for cascade selectivity and diffusion of reactants and intermediates.

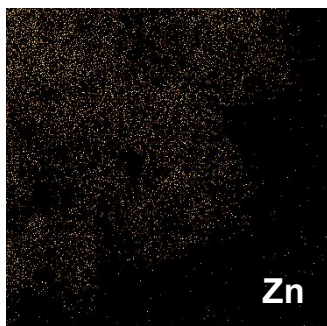


Figure S11. Zn EDX elemental map of Pd@N-ZDC@PTA-mSiO₂.

Detailed description for TEM, STEM images and EDX analysis:

The TEM, STEM images and corresponding EDX analysis of Pd@N-ZDC@PTA-mSiO₂ single catalyst were shown in Figure 1b-I, respectively. TEM images (Figure 1 b-c) further confirmed the microporous core around mesoporous shell, and crystalline Pd nanoparticles with the size of 2.5 nm. The STEM images (Figure 1d) showed the highly dispersed particle size, clear core@shell structure and uniform element distribution. Moreover, the Pd was uniformly distributed in C core, and the overlay images of C/Si and C/W showed that Si uniformly surrounded C. These results not only verified the successful fabrication of core@shell nanostructure, but also confirmed that Pd and N-doped sites were confined in C core and the large acid molecule only loaded within the mesoporous SiO₂ shell.

Detailed description for NH₃-TPD and CO₂-TPD test:

The acidic and basic properties of Pd@N-ZDC@PTA-mSiO₂ were separately investigated by tests of temperature programmed NH₃ desorption (NH₃-TPD, see Figure 2a) and temperature programmed CO₂ desorption (CO₂-TPD, see Figure 2b). For the test of NH₃-TPD, the desorption peak (maximum 519 °C) in the temperature range of 450 ~ 600 °C and peaks from 280 ~ 450 °C (Figure 2a) indicated relatively strong acid sites derived from PTA, while the peak from 50 ~ 230 °C was weak acid sites caused by the interaction between the PTA and mesostructured SiO₂. For CO₂-TPD measurements, the peak at around 116 °C originated from a weak base site was probably associated with the N-H species in N-ZDC. The desorption peak at 320 ~ 617 °C was strong base characteristic, mainly due to the pyridinic N and pyrrolic N in N-ZDC.

Detailed description for XPS:

Various interactions were confirmed by the XPS spectrum of both Pd@N-ZDC@PTA-mSiO₂ and Pd@N-ZDC@mSiO₂ shown in Figure 2c and 2d. Two peaks with binding energies of 334.9 eV (Pd 3d_{5/2}) and 340.4 eV (Pd 3d_{3/2}) shown in Figure

2c verified the existence of metallic Pd. As shown in Figure 2d, the N 1s XPS spectrum showed that three peaks at 398.8, 400.3, and 401.4 eV of Pd@N-ZDC@PTA-mSiO₂ could be assigned to pyridinic N, pyrrolic N, and graphitic N, respectively.